DOI: 10.1002/marc.((insert number)) ((or ppap., mabi., macp., mame., mren., mats.))

Communication

Heparin-mimicking sulfonated polymer nanoparticles *via* RAFT polymerisation-induced self-assembly[a]

Pratik Gurnani, Caroline P. Bray, Robert A. E. Richardson, Raoul Peltier, Sébastien Perrier*

P. Gurnani. C.P. Bray, R.A.E. Richardson, Dr. R. Peltier
Department of Chemistry, University of Warwick, Gibbet Hill Road, Coventry, CV4 7AL, UK

E-mail: s.perrier@warwick.ac.uk
Prof. S. Perrier
Department of Chemistry, University of Warwick, Gibbet Hill Road, Coventry, CV4 7AL, UK
Warwick Medical School, University of Warwick, Gibbet Hill Road, Coventry, CV4 7AL, UK
Faculty of Pharmacy and Pharmaceutical Sciences, Monash University, 381 Royal Parade, Parkville, VIC 3052, Australia.

Abstract:

Heparin plays a significant role in wound-healing and tissue regeneration applications, through stabilisation of fibroblast growth factors (FGF). Risks associated with batch-to-batch variability and contamination from its biological sources have led to the development of synthetic highly sulfonated polymers as promising heparin mimics. In this work, a systematic study of an aqueous polymerisation-induced self-assembly (PISA) of styrene from poly(2-acrylamido-2-methylpropane sodium sulfonate) (P(AMPS)) macro-RAFT agents produced a variety of spherical heparin mimicking nanoparticles, which were further characterised with light scattering and electron microscopy techniques. None of the nanoparticles tested showed toxicity against mammalian cells, however significant haemolytic activity was observed. Nonetheless, the heparin mimicking nanoparticles outperformed both heparin and linear

[a] **Supporting Information** ((bold)) is available online from the Wiley Online Library or from the author.

P(AMPS) in cellular proliferation assays, suggesting increased bFGF stabilisation efficiencies possibly due to the high density of sulfonated moieties at the particle surface.

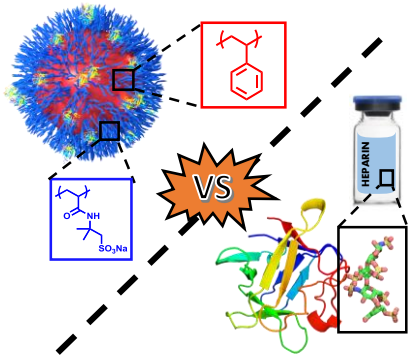

1. Introduction

Heparin is an endogenous highly sulphated polysaccharide imperative to many biological processes such as; anticoagulation, protein binding and the anti-inflammatory response.[1-3] Its biological activity is typically associated with its high charge density, which allows for strong electrostatic interactions with over 400 different proteins.[4] In particular, heparins ability to bind to and stabilise the basic fibroblast growth factor (bFGF), and its role in aiding complexation with the receptor, has attracted significant interest due to its essential function in cell proliferation, tissue regeneration and wound healing. Despite its heavy clinical use, this versatile polysaccharide can only be sourced from animal tissues (typically bovine and porcine), raising major biological safety concerns (virus contamination and large batch-batch variation/variable patient response). To overcome these challenges, researchers have studied the bFGF stabilisation efficiency of a variety of linear polysulfated/sulfonated heparin mimics, including sulfated glycopolymers, polyaromatics and polystyrenes and polyacrylamides.[5-9] For example, Maynard and co-workers recently showed 200% proliferative activity (similar to heparin + bFGF) of human dermal fibroblast cells after addition of bFGF stabilised with polystyrenesulfonate copolymers.[9]

Nanoparticles (NPs) are now well established in biomedicine for enhanced drug delivery,[10] bio-imaging[11] and diagnostics applications.[12] Their large size promotes extended circulation times and in the case of cancer treatment, they demonstrate passive tumour accumulation *via* the enhanced permeability and retention (EPR) effect.[13, 14] Furthermore, their high surface area can be functionalised with a broad range of moieties, making them ideal candidates for protein binding.[15] Although the synthesis of sulfonated/sulfated polymeric NPs has already been explored,[16-18] only one report exists on synthetic heparin mimicking NPs as growth factor stabilisers.[19] Koide *et al*. recently reported a library of polymeric NPs based on glycosylated

sulfated/sulfonated polyacrylamides able to stabilise a vascular endothelial growth factor ($VEGF_{165}$) which outperformed heparin in protein binding and anti-angiogenic experiments.[19] This pioneering study revealed huge potential for NP heparin mimics, but as of yet has not been explored in the stabilisation of bFGF.

NP's designed with advanced controlled radical polymerisation techniques, such as reversible addition fragmentation chain transfer mediated (RAFT) polymerisation induced self-assembly (PISA) can be exploited to overcome these challenges.[20, 21] PISA is typically performed through chain extension of a solvophilic macro-RAFT agent with either: a solvophilic monomer which when polymerised becomes solvophobic (RAFT dispersion polymerisation); or a solvophobic monomer (RAFT emulsion polymerisation).[22-24] This results in the formation of sterically stabilised, diblock copolymer core-shell NPs, where the particle surface is decorated with the solvophilic block of the stabilising macro-RAFT agent. Using this approach many parameters such as particle size, and stabiliser chain length can be modified, hence most PISA studies focus on nano-object synthesis and morphology control.[25-28] However, this synthetic approach has also been used for a wide range of applications. For instance, Whittaker and co-workers reported polyethylene glycol (PEG) coated NPs, copolymerised with a ^{19}F containing monomer synthesised *via* PISA for an *in vitro* cellular uptake study using magnetic nuclear resonance (MRI).[29] Furthermore, Ladmiral *et al*. reported PISA using a galactose functional monomer to enhance delivery of a model drug *via* cell surface lectin binding.[30] We have recently reported synthesis of polyacrylamide coated NPs *via* RAFT emulsion polymerisation, and their use as micro-RNA vectors and their *in vivo* biodistribution.[23, 31] Outside of biological applications, Armes and co-workers recently reported the synthesis of sulfated NPs *via* PISA both in dispersion and emulsion to further understand NP occlusion in calcite and zinc oxide crystals.[32, 33] Due to the highly sulfated nature of the above NPs, we envisaged that similar systems may be able to act as heparin mimics. However, to the best of our knowledge, there are

no reports of synthetic heparin mimicking NPs specifically applied to bFGF stabilisation, or indeed any other growth factor than $VEGF_{165}$.[19]

Herein we report the synthesis of a series of heparin mimicking core-shell NPs *via* RAFT mediated PISA of styrene from poly(2-acrylamido-2-methyl propane sulfonic acid) (P(AMPS)) macro-RAFT agents. The NPs were characterised *via* dynamic light scattering and electron microscopy. Their toxicity and membrane (haemolytic) activity was evaluated *in vitro* on murine embryonic fibroblast cells (NIH-3T3) and erythrocytes, respectively. Finally the bFGF stabilisation efficiency was determined through an *in vitro* proliferation assay using IL-3 dependent murine pro B cells (BaF3), which are engineered to over-express FGF receptors and do not produce heparin themselves.

2. Results and Discussion

2.1 Synthesis of linear polymers

Firstly, a series of three P(AMPS) homopolymers (DP20, DP50 and DP100) were prepared *via* aqueous RAFT polymerisation at 90°C using BDMAT as chain transfer agent, and VA-086 as thermal initiator (Figure 1A).[34] All three polymers had narrow molar mass distributions ($Đ$ < 1.2; **Error! Reference source not found.**) with similar experimental and theoretical molecular weights determined *via* ^{1}H NMR spectroscopy. Molecular weights determined by aqueous SEC deviated slightly from the theoretical values, likely due to the differences in hydrodynamic volume of the P(AMPS) homopolymers with the poly(ethyleneglycol) calibration. (**Error! Reference source not found.**-S3; **Error! Reference source not found.**).

2.2 Preliminary synthesis

Since P(AMPS) macro-RAFT agent synthesis was carried out in water and reached full monomer conversion, emulsion polymerisations could be performed directly without macro-RAFT agent purification. In a preliminary NP synthesis, $P(AMPS)_{50}$ was diluted in distilled water, and directly chain extended with styrene (5 wt % monomer; 450 units) at 80°C, using ACVA as a thermal initiator, 1 mM $P(AMPS)_{50}$ and 400 RPM stirring (**Error! Reference source not found.**; Figure 1A). The reaction was sampled periodically for 8 h to follow conversion, molar mass and particle size evolution over time. Between 0 - 1 h, negligible monomer conversion was observed (determined *via* gravimetry, Figure 1E), likely due to the low aqueous styrene concentration prior to micellisation. However after 1 h, both monomer conversion and particle size (measured with DLS; Figure 1C) rapidly increased, suggesting the formation of nano-objects and transport of styrene monomer into the growing particles. Both particle size and monomer conversion plateaued after 6 h at 78.5 nm and 96% respectively, indicating completion of the reaction. It should be noted that the latter time points exhibited artificial conversion values greater than 100%, we anticipate this is due to small weighing errors associated with the scale and volume of both the polymerisation and the samples taken. TEM analysis of the final latex (t = 8 h) revealed spherical NPs (Figure 1F) with relatively high polydispersity not revealed by DLS (PDi = 0.052; **Error! Reference source not found.** – *Latex 1*), possibly due to skewed sensitivity for larger species in light scattering. The polydispersity may be attributed to the ionic macro-RAFT agents reducing chain extension efficiency, affecting the uniformity of particle growth by electrostatic repulsion of similarly charged species in the aqueous phase.[35] This finding may also be attributed to the swollen corona in DLS measurements, which may artificially decrease the resulting PDi in comparison to TEM, in which the corona is fully collapsed. The highly amphiphilic block copolymer NPs were insoluble in traditional SEC eluents for polystyrene characterisation (THF, $CHCl_3$), therefore analyses were performed in DMF eluent with 0.1 wt % LiBr with polar columns. Since PS is known to swell in DMF and is not ideal for molecular weight determination, SEC

chromatograms were only used to qualitatively assess molecular weight evolution and macro-RAFT agent consumption. Using these, a clear increasing trend in molar mass over time was observed (Figure 1D), suggesting chain extension from $P(AMPS)_{50}$ had indeed occurred, however, some macro-RAFT agent remained unconsumed. Nonetheless, the highly negative zetapotentials of the NPs (-56.4 mV), suggests a dense sulfonated polymeric shell at the NP surface.

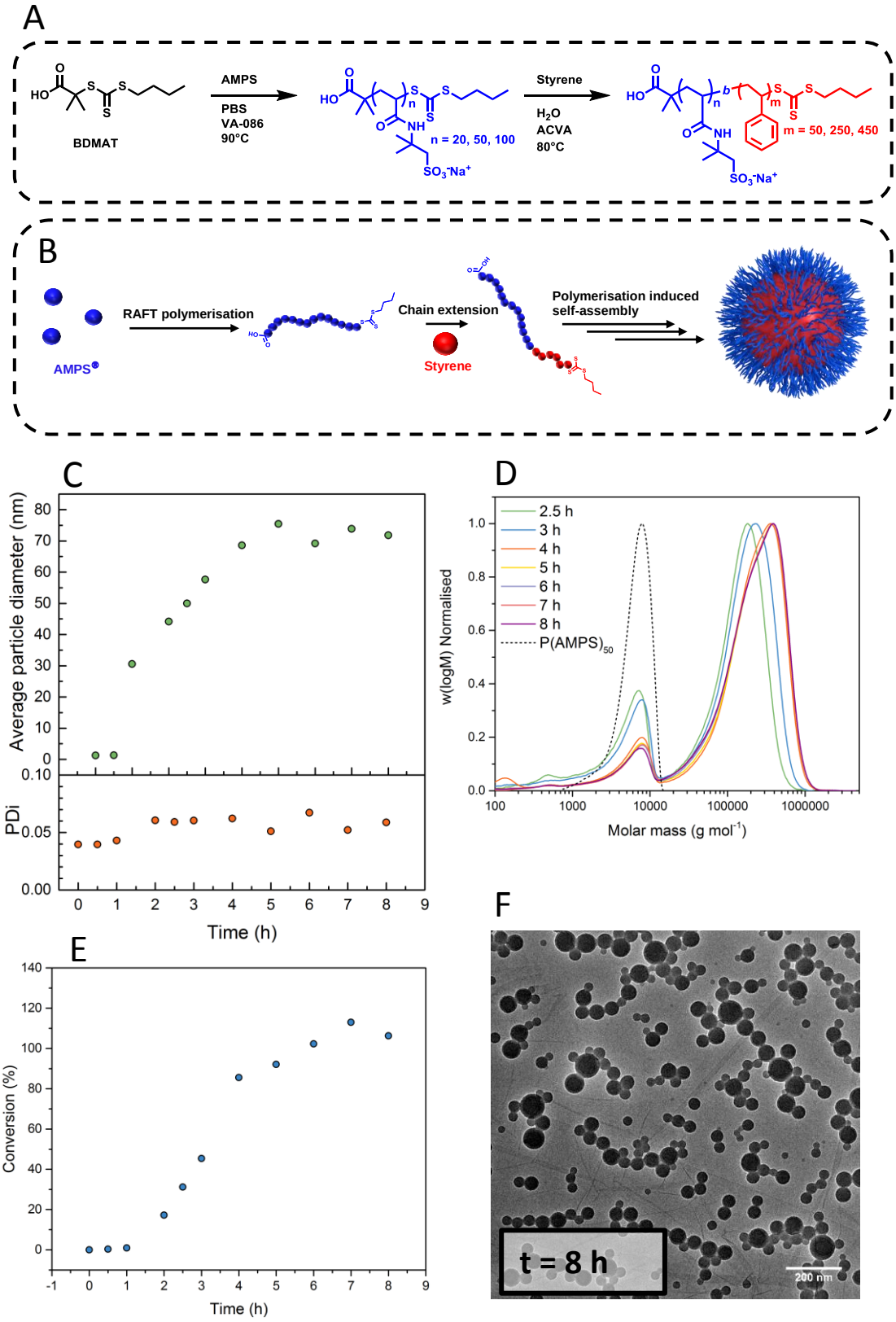

Figure 1 General synthesis scheme (A) and schematic representation (B) for the preparation of P(AMPS) macro-RAFT agents, and subsequent PISA *via* chain extension with styrene to generate P(AMPS) coated nanoparticles. Kinetic data for *Latex 1* (C) particle diameter (green

circles) and polydispersity index (red circles) as measured *via* DLS, (D) molar mass evolution of the dissolved nanoparticle unimers as measured *via* DMF SEC (E) styrene conversion as measured *via* gravimetric techniques and (F) representative TEM image at 8 h time point.

2.3 Systematic study

A systematic study on initiator type, temperature, initiator concentration, stirring speed, polystyrene DP, P(AMPS) DP and hydrophobic monomer type was then performed to improve nanoparticle polydispersity and control particle size. It should be noted that many of the latexes described below were completely insoluble in the DMF + 0.1 wt % LiBr SEC eluent, therefore for clarity only the particle size via DLS and TEM is discussed. Full characterisation and reaction conditions can be found in the supplementary information (Table S2).

2.3.1. Effect of initiator

The above-mentioned polymerisation was repeated using similar conditions but replacing ACVA (*Latex 1*) with VA-086 (*Latex 2*) and VA-057 (*Latex 3*). To account for the different 10 h half-life temperatures, the concentration of each initiator was adjusted such that the same number of radicals was generated within 6 h (Equation S2 and S3). Interestingly, the NPs synthesised with VA-086 were larger (94.2 nm) than with ACVA (78.5 nm), while those with VA-057 were smaller (59.6 nm). It is likely that as a neutral initiator VA-086 impart less electrostatic stabilisation to the growing particles resulting in fewer larger particles comprised of a higher number of polymer chains. A charged initiator, ACVA, was therefore used for all future polymerisations as no clear differences other than particle size were observed. [36, 37]

2.3.2. Effect of temperature

Similarly, the preliminary polymerisation at 80°C (*Latex 1)* was repeated at both 70°C (*Latex 4*) and 90°C (*Latex 5),* again with adjusted amounts of initiator as detailed above. At 70°C, only 71% conversion was attained, while at higher temperatures (80 and 90°C) monomer conversions higher than 90% were achieved likely due to higher propagation rates. Both temperatures yielded larger nanoparticles (91.4 nm at 70°C and 100.4 nm at 90°C). The difference at 70°C, could be explained by a decreased solubility of styrene during the early phase of the emulsion polymerisation, resulting in fewer macro-RAFT agents being chain extended, resulting in less colloidal stability.[38] At 90°C the increase in size could however be attributed to particle-particle coalescence at high temperatures.[39]

2.3.3. Effect of initiator concentration

By increasing the concentration of initiator (ACVA) (*Latex 1*; $[CTA]_0/[I]_0$ = 4.65) to double (*Latex 6*; $[CTA]_0/[I]_0$ = 2.33) and quadruple (*Latex 7*; $[CTA]_0/[I]_0$ = 0.93) the original amount, only a small increase in particle size was observed (78.5 nm (*Latex 1*) to approximately 95 nm for both concentrations). In both cases it is likely that an increased number of radicals may only result in more termination in the aqueous phase, thus leaving the effective radical concentration in the growing particles unaffected by $[I]_0$.

2.3.4. Effect of stirring speed

Increasing the stirring speed from 400 RPM (*Latex 1*) to 800 RPM (*Latex 8*) and 1200 RPM (*Latex 9*) resulted in larger NP diameters, (128.5 nm (800 RPM) and 157.7 nm (1200 RPM)). The faster, and possibly asymmetrical agitation (1200 RPM) may promote inter-particle coalescence, and therefore larger diameters.[40] Transmission electron micrographs of these NPs

however revealed uniform suspensions at 800 rpm, which most likely had uniform stirring. This stirring speed was therefore used for all future experiments.

2.3.5 Effect of polystyrene chain length

It has been widely reported that the balance of hydrophilic and hydrophobic chain length can heavily influence particle size and morphology in PISA formulations.[21] It was possible to modify the hydrophobic length (core forming block) by either increasing $[P(AMPS)_{50}]_0$ or reducing $[Styrene]_0$ in the emulsion polymerisations. This was attempted by targeting a polystyrene core with a DP of 250 (*Latex 10* and *Latex 12*) and 50 (*Latex 11* and *Latex 13*) compared to the *Latex 8* (DP_{target} = 450) by reducing $[Styrene]_0$ or increasing $[macro\text{-}RAFT]_0$. Targeting a DP of 250 both gave smaller NPs, 120.7 nm and 92.4 nm for $[Styrene]_0$ equal to 250 and 50 mM, respectively, of which both phenomena have been previously reported for similar systems.[24, 35] Further decreasing the DP_{target} to 50 however resulted in the absence of nano-object formation, suggesting that this was below the critical hydrophobic chain length for self-assembly using this type of anionic macro-RAFT agent. If compared to non-ionic stabilisers however, many reports indicate that very short hydrophobic chain lengths are able to induce micellisation, e.g below DP20.[25]

2.3.6 Effect of P(AMPS) chain length

Using the synthesised homopolymers $P(AMPS)_{20}$ (*Latex 15*) and $P(AMPS)_{100}$ (*Latex 16*), RAFT emulsion polymerisations analogous to *Latex 8* ($P(AMPS)_{50}$) were then performed. For the shorter macro-RAFT agent (DP = 20), a huge increase in particle size was observed (248.8 nm) compared to DP50 (120.7 nm), probably due to the reduced electrostatic stability of the growing particles, leading to coalescence. Unexpectedly, larger diameters (161.6 nm) were also observed with increased chain length (*Latex 16*, $P(AMPS)_{100}$ macro-RAFT agent). It is possible

that this higher overall charge may promote chain-chain repulsion and therefore a reduced number at the surface of the growing particles, with the total effect of less colloidal stability and larger particles. This could also improve the rate of radical entry and therefore account for the increase in NP uniformity with $P(AMPS)_{20}$ and $P(AMPS)_{100}$ stabilisers. It is also possible that the larger (DP 100 vs DP 50) swollen anionic corona is partially responsible for this increase in size observed in DLS.[41]

2.3.7. Effect of hydrophobic monomer

Finally, polymerisations were conducted replacing styrene (*Latex 8*) with *n*-butyl acrylate, another well-established monomer for emulsion polymerisations (*Latex 14*). This resulted in larger NPs (200.5 nm), which can be attributed to the poorer reinitiation of an acrylamide macro-RAFT agent with an acrylate monomer, thus reducing the number of sulfonated chains at the particle surface. It should be noted that due the low T_g of P(*n*-BA), *Latex 14* was imaged with cryo-transmission electron microscopy, instead of in the dry state.

In general, altering the conditions of polymerisation of these sulfonated systems did not dramatically affect the resulting NP size. However, stirring speed and P(AMPS) chain length had the greatest effect on particle size and polydispersity. The average diameter of all NPs synthesised was found to be comparable between DLS and TEM measurements, while all zeta-potentials remained similar (~ -55 to -65 mV) regardless of polymerisation conditions. All of the final latexes had pH values between 6.5 and 6.6 which is most probably caused by the P(AMPS) macro-RAFT agent/surface functionality. Furthermore, unlike other monomer combinations, our emulsion system only yielded spherical NPs, which was also observed by Armes and co-workers when using sulfated polymethacrylate macro-RAFT agent stabilisers.[32, 33]

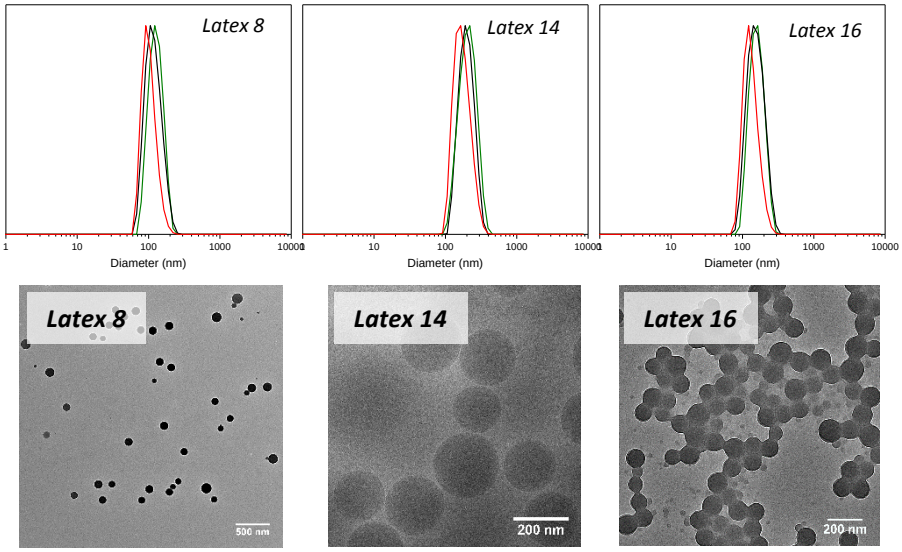

Figure 2 DLS particle size distributions (top row) (intensity = green, volume = black, number = red) measured in water at 25˚C and TEM images (bottom row) of *Latex 8*, *Latex 14* (cryogenic TEM) and *Latex 16*.

Table 1 Characterisation data for the nanoparticles used in biological studies.

				Water			PBS	
	Target structure	**Monomer**	**Conv [%][a)]**	**D_h [nm][b)]**	**PDi[c)]**	**ZP [mV][d)]**	**D_h [nm][b)]**	**PDi[c)]**
Latex 8	$P(AMPS)_{50}$-b-PS_{450}	Styrene	90	128.5	0.052	-60.3	122.0	0.072
Latex 14	$P(AMPS)_{50}$-$P(n\text{-BA})_{450}$	*n*-BA	93	200.5	0.051	-62.9	206.4	0.044
Latex 16	$P(AMPS)_{100}$-PS_{450}	Styrene	89	161.6	0.050	-61.6	165.7	0.047

[a]Determined using gravimetric techniques. [b]Determined using DLS (intensity distribution). [c]Calculated using equation S4. [d]Determined using a zetasizer.

3.4. Biological studies

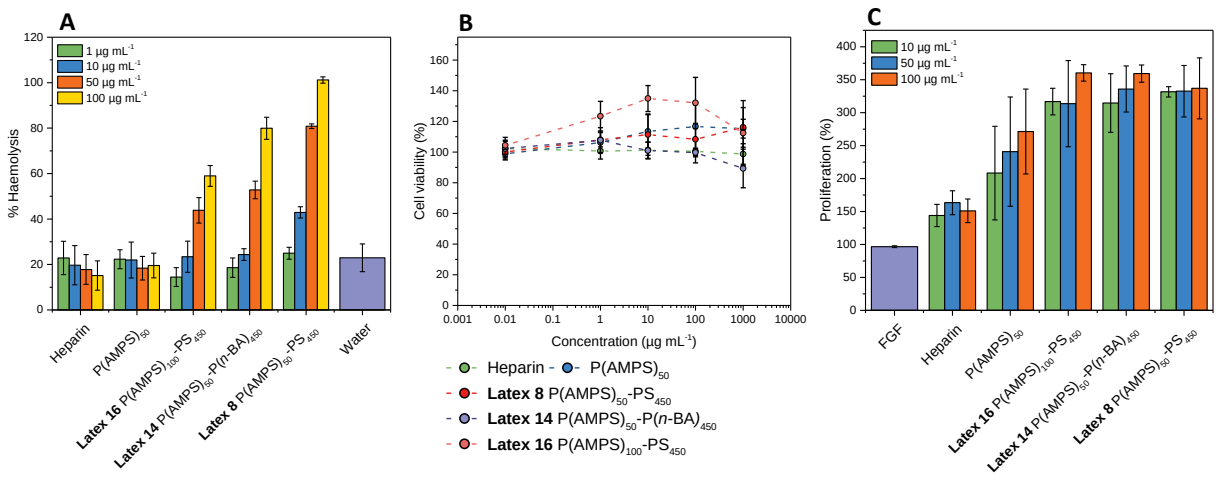

Figure 3 (A) haemolytic activity (controls of PBS and water) and (B) cytotoxicity against NIH-3T3 fibroblasts of heparin, P(AMPS)$_{50}$, *Latex 16* P(AMPS)$_{100}$-PS$_{450}$, *Latex 14* P(AMPS)$_{50}$-P(*n*-BA)$_{450}$ and *Latex 8* P(AMPS)$_{50}$-PS$_{450}$ against controls of untreated cells. (C) bFGF stabilisation as characterised via BaF3 proliferation (controls of bFGF only). Data shown represent mean ± standard deviation across triplicates from two independent experiments (N=6).

Latex 8 (P(AMPS)$_{50}$-b-PS$_{450}$), *Latex 14* (P(AMPS)$_{50}$-P(*n*-BA)$_{450}$) and *Latex 16* (P(AMPS)$_{100}$-PS$_{450}$) were chosen to study their heparin mimicking behaviour in order to isolate differences between the influence of core monomer (*n*-BA and styrene) and AMPS chain length (DP50 and DP100) on bFGF stabilisation. Additionally, these samples appeared as the most uniform from TEM images (Figure 2). Prior to these experiments, the NPs were dialysed for 48 h against a 100 kDa MWCO membrane to remove any styrene monomer, and unconsumed macro-RAFT agent which may compete against the NPs in biological studies. Importantly, the hydrodynamic diameter of the chosen latexes was comparable in PBS and in water, suggesting the NPs would be colloidally stable in biological experiments (Table 1). P(AMPS)$_{50}$ and heparin itself were also included in these experiments for comparison.

The haemolytic activity of all compounds was assessed by incubating red blood cells (1 h at 37°C) with the chosen NPs and polymers at four concentrations (100 µg mL^{-1} to 1 µg mL^{-1} in PBS) and monitoring the release of haemoglobin *via* UV spectroscopy at 414 nm. Positive (Triton-X) and negative (PBS) membrane disruption controls were also performed in parallel,

with water (5% in PBS) also used as a vehicle control. Low haemolytic activity (~20%), comparable to H_2O, were observed for heparin and $P(AMPS)_{50,}$ however much higher activity (> 50 % haemolysis) was seen for all of the NPs following the trend *Latex 8* ($P(AMPS)_{50}$-PS_{450} particles) > *Latex 14* ($P(AMPS)_{50}$-$P(n\text{-}BA)_{450}$ particles) > *Latex 15* ($P(AMPS)_{100}$-PS_{450} particles) (Figure 3A). In contrast, none of the compounds (polymers or NPs) showed acute toxicity towards murine embryonic fibroblast cells for concentrations up to 1 mg mL^{-1} (Figure 3B). This major difference between haemolysis and cytotoxicity could be due to the highly amphiphilic 'surfactant-like' nature of the particle surface-core interface, which is known to have significant membrane disruption activity.[42] The observed trend appear to support this hypothesis, as the large $P(AMPS)_{100}$ chains present on the surface of *Latex 15* will better shield erythrocytes from the PS interface compared to the shorter $P(AMPS)_{50}$. Furthermore, P(*n*-BA) is less hydrophobic than PS, and therefore NPs with these cores may be less amphiphilic, accounting for the reduction in haemolytic activity of *Latex 14*.

Finally, stabilisation of bFGF was tested using a typical proliferation assay using BaF3 cells, an IL-3 dependent murine pro B cell line which was modified to lack cell-surface heparin sulfate, and express the bFGF receptor (FGFr1c). Using this assay, heparin or a heparin mimic must be present to stabilise bFGF and promote its binding to FGFr1c receptor, thus inducing enhanced cellular proliferation. To assess this, the NPs, $P(AMPS)_{50}$ and heparin (100, 10 and 1 µg mL^{-1}) were incubated with BaF3 cells and bFGF (5 ng mL^{-1}) for 48 h, and the cellular proliferation evaluated with a cell viability assay (CellTiter-Blue®). Results were normalised to untreated cells (100%) (Figure 3C). Addition of heparin induced a small amount of proliferation (150%) which appeared independent of concentration for the range studied.[8] The linear polymer, $P(AMPS)_{50}$, resulted in approximately 250% proliferation. In contrast, all of the NPs displayed greater than 400% cellular proliferation, with no obvious differences between core composition, P(AMPS) shell length, or concentration. The full mechanism of the bFGF-

heparin-bFGFR proliferation pathway is not yet fully understood, however the key requirements are now known.[43] Heparin must induce dimerization of bFGF and simultaneously bind to bFGFR to achieve the active bFGF-heparin-bFGFR triplex required for effective proliferation.[43] A recent study by Zbinden *et al*. revealed that polymer conjugates with increased display of bFGF drastically enhanced proliferation of endothelial cells.[44] They also noted that higher densities of bFGF resulted in larger conjugate hydrodynamic volumes, which may also contribute to this effect.[44] It is probable that our large NPs with numerous surface-active P(AMPS) chains may be able to bind multiple bFGF on same species, thus improving its multivalent display. However, the smaller size and of linear $P(AMPS)_{50}$ and heparin could mean that only one, or a few of the polymers can interact with a single bFGF molecule, potentially explaining the greater cellular proliferation with the NPs. Furthermore, Garcia-Fernandez *et al*. showed that greater hydrophobicity of sulfonated linear polymers had a profound increase on bFGF stability, therefore exposed styrene from the hydrophobic NP cores may also have a similar effect.[45] It should be noted that our study evaluates cellular proliferation heparin as a function of treatment weight (e.g. 1 g of NP's vs 1 g of polymer). However, due to the higher weight proportion of PS compared to P(AMPS) in our NPs, in reality the molar concentration of sulfonated residues is exceptionally low in the NP's compared to the counterpart polymers. This highlights how the use of NP architecture could have an even greater efficacy if the number of P(AMPS) chains per particle could be elucidated, and sulfonated moieties directly compared.

Conclusions

In conclusion, we have shown a parameter screening study to generate uniform, heparin mimicking polystyrene NPs *via* aqueous RAFT emulsion polymerisation/PISA from P(AMPS)

hydrophilic macro-RAFT agents. The optimised NPs showed no cytotoxic effect against NIH-3T3 fibroblasts. However, compared to linear P(AMPS) and heparin, the NPs displayed major disruption of erythrocytes rationalised by the highly amphiphilic nature of the P(AMPS)-PS interface. Finally, all of the tested NPs exhibited much greater cellular proliferation, in comparison to heparin and linear P(AMPS) control polymers, likely due to the multivalent presentation of sulfonated chains at the NP surface. However, no apparent trends were observed between nanoparticle varieties (core properties and surface chain length) on cell proliferation. Overall, the polymerisation-induced self-assembly approach allows the facile generation of highly sulfonated NPs, and represent a promising platform for heparin mimicry in the future.

Supporting Information

Supporting Information is available from the Wiley Online Library

Acknowledgements

We thank the Royal Society Wolfson Merit Award (WM130055; SP), the European Research Council (TUSUPO 647106; SP, RP), the Engineering and Physical Sciences Research Council (PG) and Lubrizol (CPB, RAER) for financial support.

We are grateful for the Polymer Characterisation RTP for providing use of the following equipment: (SEC and Zetasizer). We are grateful to the Advanced Bioimaging RTP and Dr. Saskia Bakker for providing Cryo-TEM images.

Received: Month XX, XXXX; Revised: Month XX, XXXX; Published online:
((For PPP, use "Accepted: Month XX, XXXX" instead of "Published online")); DOI: 10.1002/marc.((insert number)) ((or ppap., mabi., macp., mame., mren., mats.))

Keywords: nanoparticle, heparin mimics, polysulfonated, growth factor

[1] P. Olczyk, L. Mencner, K. Komosinska-Vassev, *Biomed Res. Int.* **2015**, *2015*, 549417.

[2] D. Wardrop, D. Keeling, *Br. J. Haemotol.* **2008**, *141*, 757.

[3] M. Wang, Z. Lyu, G. Chen, H. Wang, Y. Yuan, K. Ding, Q. Yu, L. Yuan, H. Chen, *Chem. Commun.* **2015**, *51*, 15434.

[4] F. Peysselon, S. Ricard-Blum, *Matrix Biol.* **2014**, *35*, 73.

[5] S. J. Paluck, H. D. Maynard, *Polym. Chem.* **2017**, *8*, 4548.

[6] S. J. Paluck, T. H. Nguyen, H. D. Maynard, *Biomacromolecules* **2016**, *17*, 3417.

[7] S. J. Paluck, T. H. Nguyen, J. P. Lee, H. D. Maynard, *Biomacromolecules* **2016**, *17*, 3386.

[8] T. H. Nguyen, S. J. Paluck, A. J. McGahran, H. D. Maynard, *Biomacromolecules* **2015**, *16*, 2684.

[9] T. H. Nguyen, S. H. Kim, C. G. Decker, D. Y. Wong, J. A. Loo, H. D. Maynard, *Nat. Chem.* **2013**, *5*, 221.

[10] T. Sun, Y. S. Zhang, B. Pang, D. C. Hyun, M. Yang, Y. Xia, *Angew. Chem., Int. Ed.* **2014**, *53*, 12320.

[11] P. Sharma, S. Brown, G. Walter, S. Santra, B. Moudgil, *Adv. Colloid Interface Sci.* **2006**, *123*, 471.

[12] I. Brigger, C. Dubernet, P. Couvreur, *Adv. Drug Del. Rev.* **2012**, *64*, 24.

[13] J. Fang, H. Nakamura, H. Maeda, *Adv. Drug Del. Rev.* **2011**, *63*, 136.

[14] H. Maeda, J. Wu, T. Sawa, Y. Matsumura, K. Hori, *J. Controlled Release* **2000**, *65*, 271.

[15] P. Ke, S. Lin, W. J. Parak, T. P. Davis, F. Caruso, *ACS Nano* **2017**.

[16] S. B. Brijmohan, S. Swier, R. A. Weiss, M. T. Shaw, *Ind. Eng. Chem. Res.* **2005**, *44*, 8039.

[17] N. Yeole, D. Hundiwale, T. Jana, *J. Colloid Interface Sci.* **2011**, *354*, 506.

[18] N. Isahak, J. Sanchez, S. Perrier, M. J. Stone, R. J. Payne, *Organic & Biomolecular Chemistry* **2016**, *14*, 5652.

[19] H. Koide, K. Yoshimatsu, Y. Hoshino, S.-H. Lee, A. Okajima, S. Ariizumi, Y. Narita, Y. Yonamine, A. C. Weisman, Y. Nishimura, N. Oku, Y. Miura, K. J. Shea, *Nat. Chem.* **2017**, *9*, 715.

[20] P. B. Zetterlund, S. C. Thickett, S. Perrier, E. Bourgeat-Lami, M. Lansalot, *Chem. Rev.* **2015**, *115*, 9745.

[21] S. L. Canning, G. N. Smith, S. P. Armes, *Macromolecules* **2016**, *49*, 1985.

[22] P. Gurnani, A. M. Lunn, S. Perrier, *Polymer* **2016**, *106*, 229.

[23] C. K. Poon, O. Tang, X.-M. Chen, B. T. T. Pham, G. Gody, C. A. Pollock, B. S. Hawkett, S. Perrier, *Biomacromolecules* **2016**, *17*, 965.

[24] C. J. Ferguson, R. J. Hughes, D. Nguyen, B. T. Pham, R. G. Gilbert, A. K. Serelis, C. H. Such, B. S. Hawkett, *Macromolecules* **2005**, *38*, 2191.

[25] J. L. d. l. Haye, X. Zhang, I. Chaduc, F. Brunel, M. Lansalot, F. D'Agosto, *Angew. Chem. Int. Ed.* **2016**, *55*, 3739.

[26] S. Dong, W. Zhao, F. P. Lucien, S. Perrier, P. B. Zetterlund, *Polym. Chem.* **2015**, *6*, 2249.

[27] W. Zhang, F. D'Agosto, O. Boyron, J. Rieger, B. Charleux, *Macromolecules* **2012**, *45*, 4075.

[28] L. A. Fielding, M. J. Derry, V. Ladmiral, J. Rosselgong, A. M. Rodrigues, L. P. D. Ratcliffe, S. Sugihara, S. P. Armes, *Chem. Sci.* **2013**, *4*, 2081.

[29] W. Zhao, H. T. Ta, C. Zhang, A. K. Whittaker, *Biomacromolecules* **2017**, *18*, 1145.

[30] V. Ladmiral, M. Semsarilar, I. Canton, S. P. Armes, *J. Am. Chem. Soc.* **2013**, *135*, 13574.

[31] C. K. Poon, O. Tang, X. M. Chen, B. Kim, M. Hartlieb, C. A. Pollock, B. S. Hawkett, S. Perrier, *Macromol. Biosci.* **2017**, *17*, 1600366.

[32] Y. Ning, L. A. Fielding, L. P. D. Ratcliffe, Y.-W. Wang, F. C. Meldrum, S. P. Armes, *J. Am. Chem. Soc.* **2016**, *138*, 11734.

[33] Y. Ning, L. A. Fielding, T. S. Andrews, D. J. Growney, S. P. Armes, *Nanoscale* **2015**, *7*, 6691.

[34] C. Bray, R. Peltier, H. Kim, A. Mastrangelo, S. Perrier, *Polym. Chem.* **2017**, *8*, 5513.

[35] I. Chaduc, A. Crepet, O. Boyron, B. Charleux, F. D'Agosto, M. Lansalot, *Macromolecules* **2013**, *46*, 6013.

[36] K. Y. van Berkel, G. T. Russell, R. G. Gilbert, *Macromolecules* **2003**, *36*, 3921.

[37] C. S. Chern, S. Y. Lin, S. C. Chang, J. Y. Lin, Y. F. Lin, *Polymer* **1998**, *39*, 2281.

[38] I. Capek, S. Y. Lin, T. J. Hsu, C. S. Chern, *J. Polym. Sci., Part A: Polym. Chem.* **2000**, *38*, 1477.

[39] E. Gonzalez, C. Tollan, A. Chuvilin, M. J. Barandiaran, M. Paulis, *ACS Appl. Mater. Interfaces* **2012**, *4*, 4276.

[40] M. Nomura, M. Harada, W. Eguchi, S. Nagata, *J. Appl. Polym. Sci.* **1972**, *16*, 835.

[41] N. Yeole, D. Hundiwale, *Colloids Surf. Physicochem. Eng. Aspects* **2011**, *392*, 329.

[42] B. Isomaa, A. Engblom, H. Hägerstrand, *Toxicology* **1988**, *48*, 285.

[43] S. Sarabipour, K. Hristova, *Nat. Commun.* **2016**, *7*, 10262.

[44] A. Zbinden, S. Browne, E. I. Altiok, F. L. Svedlund, W. M. Jackson, K. E. Healy, *Biomater. Sci.* **2018**.

[45] L. García-Fernández, M. R. Aguilar, M. M. Fernández, R. M. Lozano, G. Giménez, J. S. Román, *Biomacromolecules* **2010**, *11*, 626.